Bioorganic & Medicinal Chemistry 18 (2010) 4453–4458

Contents lists available at ScienceDirect

Bioorganic & Medicinal Chemistry

journal homepage: www.elsevier.com/locate/bmc

Controlled release of PEG chain from gold nanorods: Targeted delivery to tumor

Takuro Niidome [a,b,c,*], Akira Ohga [a], Yasuyuki Akiyama [a], Kazuto Watanabe [a], Yasuro Niidome [a], Takeshi Mori [a,b], Yoshiki Katayama [a,b]

[a] Department of Applied Chemistry, Faculty of Engineering, Kyushu University, 744 Motooka, Nishi-ku, Fukuoka 819-0395, Japan
[b] Center for Future Chemistry, Kyushu University, 744 Motooka, Nishi-ku, Fukuoka 819-0395, Japan
[c] PRESTO, Japan Science and Technology Corporation, Kawaguchi 332-0012, Japan

ARTICLE INFO

Article history:
Received 17 March 2010
Revised 20 April 2010
Accepted 21 April 2010
Available online 28 April 2010

Keywords:
Gold nanorods
Peptide
Photothermal effect
Polyethyleneglycol
Tumor-targeting
Urokinase-type plasminogen activator

ABSTRACT

Gold nanorods exhibit strong absorbance of light in the near infrared region, which penetrates deeply into tissues. Since the absorbed light energy is converted into heat, gold nanorods are expected to act as a contrast agent for in vivo bioimaging and as a thermal converter for photothermal therapy. To construct a gold nanorod targeted delivery system for tumor a peptide substrate for urokinase-type plasminogen activator (uPA), expressed specifically on malignant tumors, was inserted between the PEG chain and the surface of the gold nanorods. In other words, we constructed PEG–peptide-modified gold nanorods. After mixing the gold nanorods with uPA, the PEG chain was released from the surface of the gold and subsequently nanorod aggregation took place. The formation of the aggregation was monitored as a decrease in light absorption at 900 nm. Tumor homogenate induced a significant decrease in this absorption. Larger amount of the PEG–peptide-modified gold nanorods bound to cells expressing uPA in vitro compared with control gold nanorods, which had scrambled sequence of the peptide. The PEG–peptide-modified gold nanorods showed higher accumulation in tumor than the control after they were injected intravenously into tumor-bearing mice, however, the density of the peptide on the surface of the gold nanorods was a key factor of their biodistributions. This targeted delivery system, which responds to uPA activity, is expected to be a powerful tool for tumor bioimaging and photothermal tumor therapy.

1. Introduction

The development of targeted delivery systems for nanoparticles such as liposomes, polymer micelles, quantum dots, magnetite nanoparticles and gold nanoparticles to facilitate the bioimaging of target sites and for therapy is an important area of research. To deliver the nanoparticles specifically, an extensive range of strategies have been reported.[1] Traditional tumor targeting strategies relay on a phenomenon known as the enhanced permeability and retention (EPR) effect. Tumors contain defective and permeable blood vessels that allow particles to accumulate inside them, a process known as passive targeting.[2,3] Active targeting involves conjugating molecules that have affinity for the cell surface. Antibodies, folate, RGD peptide, transferrin and aptamers have been studied as active targeting molecules.[1,4–12]

Recently, new strategies for the development of tumor targeting systems that respond to the unique environment of the tumor have been studied. Since the extracellular pH of the tumor is slightly acidic (pH 6.5–7.2),[13] pH responsive polymers whose conformations are changed when exposed to acidic pH have been used as carriers that can release drug in the tumor specifically.[14–16] The polymer forms a stable micelle structure in neutral conditions. Once the pH decreases to below pH 7, the hydrophobicity of the polymer is decreased. As a consequence, the micelles swell and the entrapped drug in the micelles is released. Protease activity is also considered to be a feature of the unique environment of the tumor. Matrix metalloproteases (MMPs) are specifically expressed in the tumor. A conjugate of methotrexate and dextran via a peptide linker that can be cleaved by MMP-2 and MMP-9 has been developed.[17–19] Such a protease-responding drug retention system has been expanded to deliver genes,[20] magnetite nanoparticles,[21] gold nanoparticles[22] and quantum dots to tumor.[23] These systems work not only as a tumor delivery system for nanoparticles, and modified drugs attached to the nanoparticles, but also as bioimaging modalities for use in magnetic resonance imaging and fluorescence imaging of tumors. Such a theragnostic system is expected to be used as a novel technology in medicine in the next generation. In addition, the protease urokinase-type

Abbreviations: CTAB, hexadecyltrimethylammonium bromide; EPR, enhanced permeability and retention; ICP-MS, inductively coupled plasma mass spectrometry; MMP, matrix metalloprotease; PBS, phosphate buffered saline; PEG, polyethylene glycol; TBS, 50 mM Tris–HCl buffer, pH 7.4 containing 100 mM NaCl; TEM, transmission electron microscopy; uPA, urokinase-type plasminogen activator.

* Corresponding author. Tel./fax: +81 92 802 2851.
E-mail address: niidome.takuro.655@m.kyushu-u.ac.jp (T. Niidome).

0968-0896/$ - see front matter © 2010 Elsevier Ltd. All rights reserved.
doi:10.1016/j.bmc.2010.04.070

plasminogen activator (uPA) is expected to be widely expressed on malignant tumors.[24] Kinoh et al. developed the oncolytic Sendai virus (SeV) vector, in which the substrate sequence (SGRS) of the uPA was inserted into the tryptic cleavage site of F0, which triggers membrane fusion activity in the infected cells.[25,26] The resultant uPA-responsive SeV showed syncytia formation in uPA-expressing PC-3 cells. Subsequently, extensive cell death through massive cell-to-cell spreading without significant dissemination to the surrounding noncancerous tissue was observed in vivo. Thus, the substrate peptide of uPA is also expected to be a promising candidate that can function as a sensor to activate drug/gene carriers at the tumor site, in addition to acting as a substrate for MMPs.

Among the nanoparticles rod-shaped gold nanoparticles, or gold nanorods as they are commonly called, are being developed as a functional nanodevice that works in tissue. The gold nanorods have two distinctive adsorption bands corresponding to the transverse and longitudinal surface plasmon oscillations of free electrons in the visible (~520 nm) and near infrared (~900 nm) regions, respectively.[27,28] Since the near infrared light is ideally suited for in vivo imaging and laser therapy due to its high tissue penetration,[29] the gold nanorods are expected to act as contrast agents for in vivo bioimaging. They are also expected to function as thermal converters for photothermal therapy because they exhibit a photothermal effect, that is, the absorbed light energy is efficiently converted into heat.[30] To enable the gold nanorods to used for such medical applications, they have been modified with polyethylene glycol (PEG)[31,32] and detailed biodistribution studies have been carried out after their intravenous injection into mice.[32,33] Actually, the PEG-modified gold nanorods have been employed as a contrast agent for in vivo bioimaging systems using near infrared laser light.[34–36] Demonstrations of photothermal cancer therapy using gold nanorods as a photothermal converter have also been reported by several groups.[36,37]

Targeting gold nanorods to a specific site is a critical aspect of bioimaging using gold nanorods as a contrast agent and for achieving efficient photothermal therapy without side effects, especially after intravenous injection. The primary objective of the present study was to construct a gold nanorod targeted delivery system that responds to protease activity, especially uPA. This is expected to be a new and promising strategy for tumor targeting among several methods that have been reported.[7,11]

2. Results and discussion

2.1. Preparation of PEG–peptide-modified gold nanorods

To construct the targeted delivery system of gold nanorods responding to uPA activity, the peptide substrate of uPA was inserted between the PEG and gold surface of the PEG-modified gold nanorods. If uPA cleaves the peptide chain, PEG is released from the surface of the gold nanorods. It is then expected that the gold nanorods form an aggregation or adsorb hydrophobic materials. The peptide-inserted PEG-modified gold nanorods (PEG–peptide-modified gold nanorods) were prepared as follows. PEG-modified peptide (PEG_{5000}-LGGSGRSANAILEC) was modified with the gold nanorods through an Au–S bond by mixing the PEG–peptide with gold nanorods stabilized by CTAB at PEG/Au molar ratios of 0.1, 0.01 and 0.001. After that the remaining CTAB and excess PEG–peptide were removed by centrifugation. The resultant PEG–peptide-modified gold nanorods were designated as PEG-uPA-$NR_{0.1}$, PEG-uPA-$NR_{0.01}$ and PEG-uPA-$NR_{0.001}$.

The absorption spectra of the PEG–peptide-modified gold nanorods were measured (Fig. 1). Spectra exhibited the typical characteristics of a gold nanorod solution, that is, two surface plasmon bands at 510 and 920 nm corresponding to the transverse and longitudinal oscillation modes, respectively, were observed. The spectrum of the PEG–peptide-modified gold nanorods was similar to that of the original CTAB-stabilized gold nanorods, indicating that no aggregation of the gold nanorods had occurred after the modification. Using transmission electron microscopy (TEM), well-dispersed gold nanorods were observed and a significant shadow that originated from the PEG–peptide layers was evident around the gold nanorods (Fig. 2). Zeta potentials of the gold nanorods were measured. CTAB-stabilized gold nanorods had cationic surfaces (+28.7 ± 0.2 mV) due to the presence of adsorbed CTAB that had a quaternary amine as a hydrophilic head. In contrast, the PEG–peptide-modified gold nanorods had a nearly neutral surface. Such a neutral and hydrophilic surface made by the PEG chains contributes to reduction of non-specific interaction with blood cells and proteins, and avoidance of uptake by reticuloendothelial cells in the liver and the spleen.[31,32]

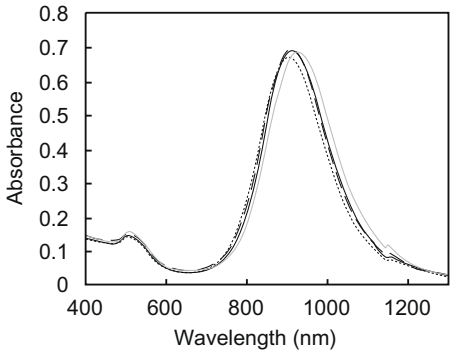

Figure 1. Gold nanorod absorption spectra. CTAB-stabilized gold nanorods (*gray line*), PEG-uPA-$NR_{0.1}$ (*solid line*), PEG-uPA-$NR_{0.01}$ (*broken line*) and PEG-uPA-$NR_{0.001}$ (*dotted line*).

Next, we evaluated the dispersion stability of the PEG–peptide-modified gold nanorods in 50 mM Tris–HCl buffer at pH 7.4 containing 100 mM NaCl (TBS) by measuring their absorbances at 900 nm (Fig. 3). PEG-uPA-$NR_{0.1}$ and PEG-uPA-$NR_{0.01}$ showed no change in absorbance after 15 min incubation in TBS at 37 °C. This indicated that no aggregation formed under such conditions. In contrast, PEG-uPA-$NR_{0.001}$ showed a dramatic decrease in absorbance immediately after the mixing of the gold nanorods with TBS. The PEG–peptide modified on the gold nanorods at PEG/Au molar ratios of 0.001 was not enough to stabilize the gold nanorods in such a physiological condition. In the present study, considering both the accessibility of uPA to the peptide moiety covered by the PEG layer on the gold surface and stability under physiological conditions, PEG-uPA-$NR_{0.01}$ was mainly employed in experiments.

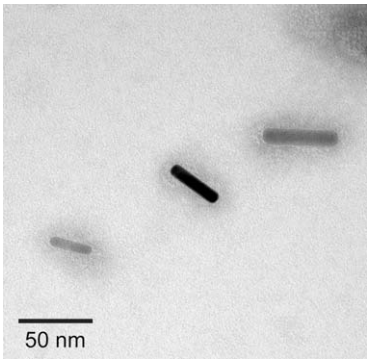

Figure 2. TEM image of PEG-uPA-$NR_{0.01}$. The PEG layer was stained with 1% phosphotungstic acid.

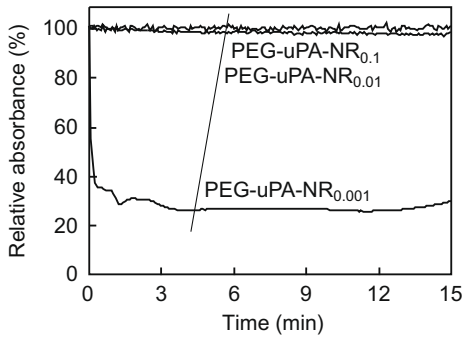

Figure 3. Dispersion stabilities of the PEG–peptide-modified gold nanorods. PEG-uPA-$NR_{0.1}$, PEG-uPA-$NR_{0.01}$ and PEG-uPA-$NR_{0.001}$ were added to TBS to give a concentration of 0.1 mM as gold atoms. Absorbance at 900 nm was monitored at 37 °C for 15 min.

2.2. Cleavage of the peptide on the gold nanorods and aggregate formation

PEG-uPA-$NR_{0.01}$ was incubated with uPA (400 nM) for 30 min, then absorption spectra were measured (Fig. 4A). After incubation a significant decrease in absorption was observed in the near infrared region, while no change was observed in the absence of uPA. Using electron microscopy, large aggregates were observed in the presence of uPA (Fig. 4B), while the gold nanorods dispersed in the absence of uPA (Fig. 4C). To examine the effect of uPA concentration on gold nanorods aggregate formation, decreases in the absorption of PEG-uPA-$NR_{0.01}$ at 900 nm after the addition of uPA (0–400 nM) were continuously monitored (Fig. 5A). The decrease was dependent on the concentration of uPA. At least 200 nM of uPA was necessary to produce a significant decrease in absorption at 5 min. In contrast, no decrease in absorption was observed when uPA was pretreated with its inhibitor, amiloride, or when peptide with scrambled sequence (LGGSGASNRAILEC) was used instead of the peptide substrate in the PEG–peptide-modified gold nanorods (Fig. 5B). These results indicated that gold nanorod aggregate formation was due to the release of PEG chains triggered by uPA that cleaved the peptide component between the PEG chain and the gold nanorods.

Next, we investigated whether the presence of uPA in tumor homogenate could be detected using the PEG–peptide-modified gold nanorods. Mouse 4T1 breast carcinoma cells, that are known to express a high level of uPA, were subcutaneously inoculated into mice. After inoculation a homogenate from the tumor was prepared. The tumor homogenate was mixed with PEG-uPA-$NR_{0.01}$ and the decrease in absorption at 900 nm was monitored (Fig. 6). It took several minutes before absorption started to decrease but a significant decrease was observed after 20 min. This might be due to a large amount of impurity that affected aggregate formation of the gold nanorods. When the homogenate was pretreated with the inhibitor, amiloride, no decrease was observed indicating that uPA-specific peptide cleavage had occurred in the reaction mixture.

2.3. Binding ability of PEG–peptide-modified gold nanorods to tumor cells in vitro

The PEG–peptide-modified gold nanorods are expected to bind with hydrophobic interaction to uPA-expressing tumor cells because the PEG chains are released from the surface of the gold. We investigated the cell-binding potential of the PEG–peptide-modified gold nanorods using 4T1 cells in vitro. PEG-uPA-$NR_{0.1}$, PEG-uPAscr-$NR_{0.1}$, PEG-uPA-$NR_{0.01}$ and PEG-uPAscr-$NR_{0.01}$ were added to the 4T1 cells, and then incubated for 24 h. The amount

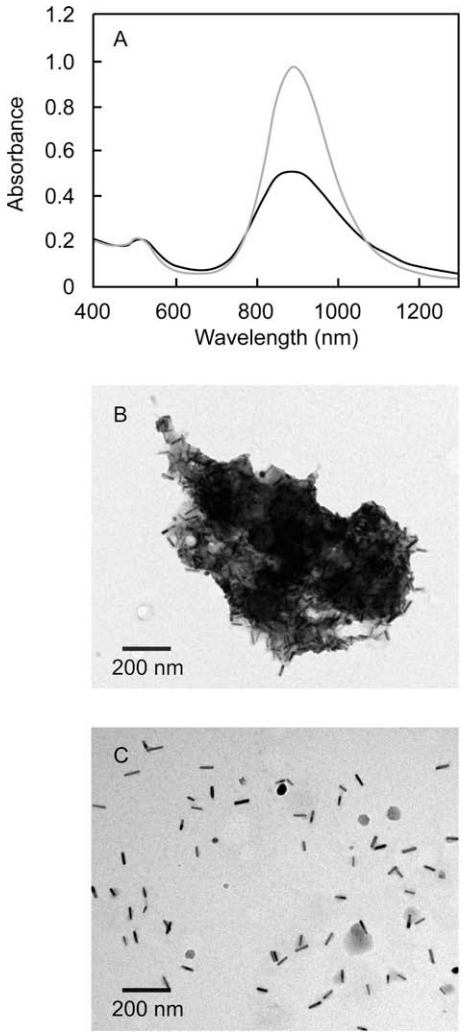

Figure 4. TEM images of gold nanorod aggregate formation after the addition of uPA. (A) Absorption spectra of PEG-uPA-$NR_{0.01}$ after incubation with 400 nM uPA in TBS at 37 °C for 30 min (*black line*) or without uPA (*gray line*). (B) TEM images of PEG-uPA-$NR_{0.01}$ incubated with 400 nM uPA at 37 °C for 30 min. (C) TEM images of PEG-uPA-$NR_{0.01}$ incubated without uPA at 37 °C for 30 min. The PEG layer was stained with 1% phosphotungstic acid.

of cell-bound gold was quantified using inductively coupled plasma mass spectrometry (ICP-MS) (Fig. 7). It was found that a larger amount of PEG-uPA-NR was bound to the cells as compared with PEG-uPAscr-NR in the case of the gold nanorods prepared at either PEG:Au molar ratios. This indicated that the PEG chains of PEG-uPA-NR were released specifically by uPA on the cells. In the case of the PEG-modified gold nanorods prepared at PEG:Au molar ratios of 0.1, the amount of gold bound to the cells was lower than that in the case for the PEG-modified gold nanorods prepared at PEG:Au molar ratios of 0.01. It was considered that the PEG chain modified to have a high density on the surface of the gold impeded access of uPA to the peptide component covered by the PEG layer, as compared with the lower density PEG chain.

2.4. Accumulation of the PEG–peptide-modified gold nanorods to tumor after intravenous injection to mice

PEG-uPA-$NR_{0.1}$, PEG-uPAscr-$NR_{0.1}$, PEG-uPA-$NR_{0.01}$ and PEG-uPAscr-$NR_{0.01}$ were intravenously injected into tumor-bearing mice. The mice were sacrificed at 72 h after injection, at which time the gold nanorods were expected to be completely cleared from

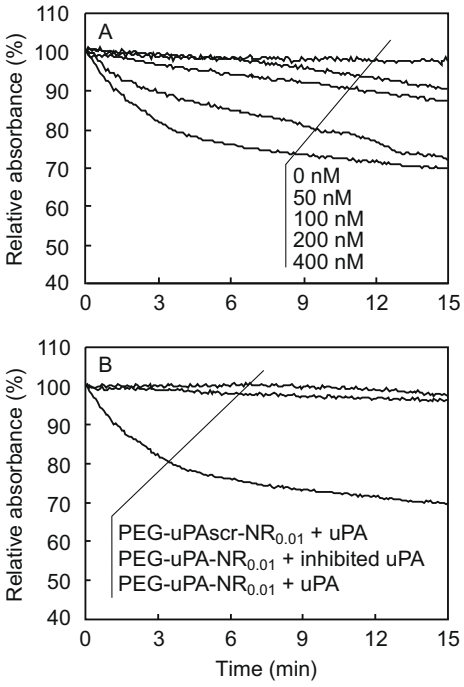

Figure 5. Decreases in light absorption of the PEG–peptide-modified gold nanorods. (A) uPA was added to PEG-uPA-$NR_{0.01}$ at several concentrations (0–400 nM) in TBS and then absorption at 900 nm was monitored at 37 °C for 15 min. (B) uPA (400 nM) pretreated with inhibitor (amiloride) was added to PEG-uPA-$NR_{0.01}$ in TBS, or uPA (400 nM) was added to PEG-uPAscr-$NR_{0.01}$ which contained a scrambled sequence of the substrate peptide in TBS. Subsequently, decreases of absorption at 900 nm were monitored at 37 °C for 15 min.

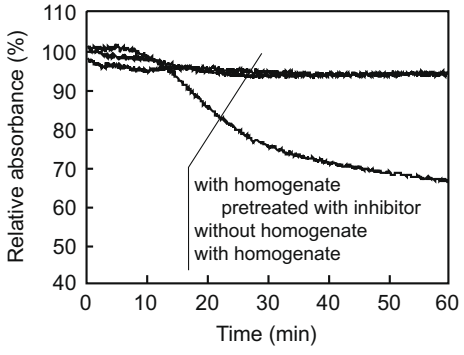

Figure 6. Decreases in the light absorption of the PEG–peptide-modified gold nanorods mediated by tumor homogenate. Tumor-bearing mice were prepared by subcutaneously inoculating 4T1 cells that are known to express a high level of uPA. Extracted tumor tissue was homogenized in TBS. The suspension was ultracentrifuged at 120,000*g* at 4 °C for 45 min and the supernatant was used for enzymatic reaction. The homogenate-alone and homogenate pretreated with the inhibitor, amiloride, was added to PEG-uPA-$NR_{0.01}$. Following this, decreases in absorption at 900 nm were monitored at 37 °C for 60 min.

the blood.[33] Tumors were collected and the amount of the gold in the tumor was quantified by ICP-MS (Fig. 8). In the case of the PEG-modified gold nanorods prepared at PEG:Au molar rations of 0.1, a higher amount of the gold was detected in PEG-uPA-NR as compared with PEG-uPAscr-NR. This finding indicates that the peptide substrate component acted as a responsive element in the retention of the gold nanorods at uPA expressing sites in tumor tissue. In the case of the PEG-modified gold nanorods prepared at a PEG:Au molar ratio of 0.01, PEG-uPAscr-NR showed a slightly higher accumulation than PEG-uPA-NR. However, the levels of accumulation of these two gold nanorod variants were appreciably lower

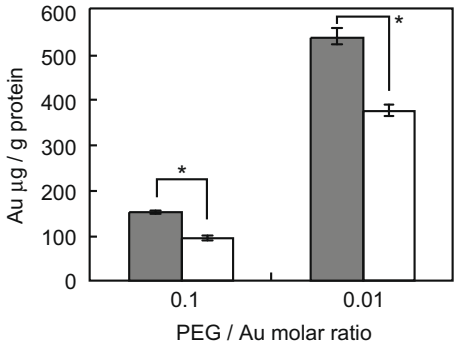

Figure 7. Binding ability of the PEG–peptide-modified gold nanorods to uPA-expressing cells. PEG-uPA-$NR_{0.1}$, PEG-uPAscr-$NR_{0.1}$, PEG-uPA-$NR_{0.01}$ and PEG-uPAscr-$NR_{0.01}$ were added to 4T1 cells and then incubated for 24 h. The amounts of gold bound to cells were quantified by ICP-MS. *Closed bars* and *open bars* indicate the amounts of bound PEG-uPA-NR and PEG-uPAscr-NR, respectively. Data represent mean values for $n = 3$ and bars are standard errors from the means. $^{*}P < 0.005$.

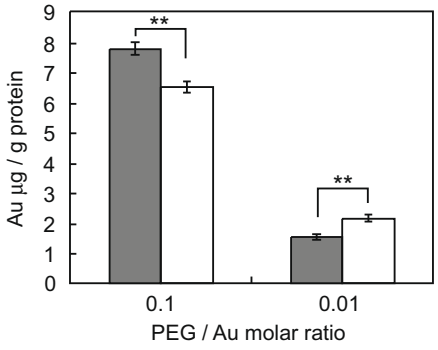

Figure 8. Accumulation of the PEG–peptide-modified gold nanorods in tumor. After intravenous injection of PEG-uPA-$NR_{0.1}$, PEG-uPAscr-$NR_{0.1}$, PEG-uPA-$NR_{0.01}$ and PEG-uPAscr-$NR_{0.01}$ into tumor-bearing mice, the mice were sacrificed at 72 h. The tumors were collected and the amount of gold in the tumor was quantified using ICP-MS. *Closed bars* and *open bars* indicate the amounts of PEG-uPA-NR and PEG-uPAscr-NR, respectively, in the tumor. Data represent mean values for $n = 3$ and the bars are standard errors of the means. $^{**}P < 0.05$.

than that of the PEG-modified gold nanorods prepared at a PEG:Au molar ratio of 0.1. However, this result is inconsistent with that obtained from the in vitro study using 4T1 cells (Fig. 7). After intravenous injection, the gold nanorods circulated in the blood stream and then a proportion of them reached tumor tissue expressing uPA. In such a situation the stealth character of the gold nanorods in the circulation, which was achieved by modifying a larger amount of the PEG chain, would strongly contribute to the EPR effect-driven accumulation of gold nanorods in the tumor as compared with the accessibility of uPA to the peptide component of the nanorod.

3. Conclusion

PEG–peptide-modified gold nanorods containing peptide substrate for uPA, which is expressed on malignant tumors, formed aggregates in response to uPA activity. This was due to the release of the PEG chain from the surface of the gold nanorod as the result of cleavage of the peptide component. Binding of the gold nanorods to uPA-expressing cells in vitro was also mediated by the cleavage of the peptide component. After intravenous injection of the gold nanorods, a larger amount of the gold was detected in the tumor as compared with the control (i.e., use of the scramble sequence replaced in the PEG–peptide-modified gold nanorods). However, the

density of the PEG–peptide on the surface of the gold was a key factor, not only in maintaining the stability of the gold nanorods under physiological conditions, but also to secure the accessibility of uPA to the peptide component covered by the PEG layer.

When the delivery system is applied to tumor imaging and photothermal tumor therapy, the absorption of the gold nanorods at the near infrared light region should be maintained. It is expected that lots of molecules such as serum and extracellular matrix proteins in the tumor tissue non-specifically bind to the surface of the gold nanorods immediately after the peptide cleavage. As a result, aggregation that decreases the absorption of the nanorods would be hindered. Further optimization of the PEG–peptide-modified gold nanorods will enable the establishment of a targeted delivery system that can be utilized to the tumor bioimaging and its therapy.

4. Experimental

4.1. Materials

Gold nanorods prepared using our previous methods were supplied by Mitsubishi Materials Corporation (Tokyo, Japan) and Dai Nippon Toryo Co. Ltd (Osaka, Japan)[38] The average length and width of the as-supplied gold nanorods were 48.8 ± 7.9 nm and 9.0 ± 1.2 nm, respectively (aspect ratio: 5.4). *N*-Hydroxy succinimide-terminated poly (ethylene glycol) (PEG) (MW ca. 5000 Da) was purchased from NOF Co., Ltd (Tokyo, Japan). uPA was purchased from Calbiochem (Darmstadt, Germany).

4.2. Synthesis of PEG–peptide conjugates

uPA peptide substrate (LGGSGRSANAILEC) and the scrambled control peptide (LGGSGASNRAILEC) were manually synthesized using Fmoc-chemistry on Rink Amide AM resin. After deprotection and cleavage from the resin, the peptides were purified by RP-HPLC. *N*-hydroxy succinimide-terminated PEG (NOF Co., Ltd (Tokyo, Japan); MW ca. 5000 Da) was reacted with the amine of the α-amino group of the amino terminal of the peptide. Subsequently the resulting PEG–peptide conjugates were dialyzed for three days.

4.3. Preparation of PEG–peptide-modified gold nanorods

The original gold nanorod solution containing CTAB was centrifuged at 14,000 *g* for 10 min), decanted and re-suspended in water to remove excess CTAB. The PEG–peptide conjugates solution was added to the gold nanorod suspension at PEG:Au molar ratios of 0.1, 0.01 and 0.001. The mixtures were stirred overnight at room temperature and centrifuged at 14,000 *g* for 10 min, decanted and re-suspended in water to remove the remaining CTAB and excess PEG–peptide conjugates. The resultant PEG–peptide-modified gold nanorods containing uPA substrate peptide, or scrambled control peptide, were designated PEG-uPA-$NR_{0.1}$, PEG-uPA-$NR_{0.01}$, PEG-uPA-$NR_{0.001}$, PEG-uPAscr-$NR_{0.1}$, PEG-uPAscr-$NR_{0.01}$ and PEG-uPAscr-$NR_{0.001}$.

4.4. Characterization of the PEG–peptide-modified gold nanorods

Absorption spectra of the gold nanorods from the visible to near infrared light region were measured with a JASCO V-670 spectrophotometer (Tokyo, Japan). Gold nanorod morphology was observed using a JOEL JEM-2010 TEM (Tokyo, Japan) after staining with 1% phosphotungstic acid. The zeta potential of the gold nanorods was evaluated using a Malvern Zetasizer Nano ZS (Malvern Instruments Ltd, WR, UK).

4.5. Enzymatic reaction

PEG-uPA-$NR_{0.01}$ (0.1 mM as gold atoms) were incubated with or without 400 nM uPA in 50 mM Tris-HCl buffer, pH 7.4 containing 100 mM NaCl (TBS) at 37 °C for 30 min. After incubation the absorption spectra were measured. In the same way PEG-uPA-$NR_{0.01}$ and PEG-uPAscr-$NR_{0.01}$ were incubated with 50–400 nM uPA or 10 μg/mL tumor homogenate. Absorbance change at 900 nm was monitored during the enzymatic reaction. As an additional control experiment, uPA pretreated with 2 mM amiloride, uPA inhibitor, at 37 °C for 1.5 h in TBS was used to distinguish uPA-mediated peptide cleavage from non-specific cleavage.

4.6. Evaluation of the cell adsorptive property in tumor cells

Mouse breast carcinoma 4T1 cells (1.0×10^6) were seeded in dishes and incubated at 37 °C for 48 h in medium (RPMI1640 containing 10% fetal bovine serum, 100 U/mL penicillin, 100 μg/mL streptomycin and 0.25 μg/mL amphotericin B [Invitrogen, CA, USA]). The dishes containing cells were maintained at 37 °C in an incubator under a 5% CO_2 atmosphere. After 48 h the medium was removed and the cells were washed with phosphate buffered saline (PBS). Three mL of the medium containing gold nanorods (0.01 mM as gold atoms) was added to the dishes and the cells were further incubated for 24 h. After removing the medium, the cells were washed with PBS and lysed in 3 mL of lysis buffer (20 mM Tris–HCl, pH 7.0 containing 0.05% Triton-X 100 and 2 mM EDTA). After collecting the suspension the protein concentration of each sample was determined using the Bradford method (Coomassie Brilliant Blue G-250 reagent; BIO-RAD Lab., CA, USA) and then the rest of the samples were lyophilized. The samples were added to approximately 4 mL aqua regia and then heated overnight at 95 °C. The organic compounds were completely oxidized and the gold was ionized. Finally, the samples were condensed by further heating at 120 °C for 2 h. The residues were dissolved in 1 mL of 0.5 M HCl. Quantitative analysis of gold was performed by inductively coupled plasma mass spectrometry (ICP-MS) using the Agilent 7500c (Agilent, CA, USA).

4.7. Animals

Male BALB/c mice (Kyudo Co., Ltd, Saga, Japan) were used in all experiments. Five-week old mice were maintained in a temperature-controlled environment at 24 °C with a 12 h light/dark cycle and were provided with drinking water and feed ad libitum. Animal experiments were performed according to the Guidelines of the Animal Care and Use Committee, Kyushu University.

4.8. Implantation of tumor cells to mice

Tumor-bearing mice were prepared as follows. 4T1 cells were injected subcutaneously into the abdomen at a dose of 4×10^6 cells in 100 μl Hank's balanced salt solution per mouse (BALB/c, male, five weeks-old, 22–26 g body weight) and allowed to grow for five days, at which time the tumors reached a size of 5–7 mm in diameter.

4.9. Preparation of tumor homogenates

Tumors were collected from tumor-bearing mice. The tumors were suspended in TBS in a ratio of 1 mL per 100 mg of tumor and homogenized using a Potter homogenizer for 30 s. The suspension was ultracentrifuged at 120,000 *g* at 4 °C for 45 min and the supernatant was used for the enzymatic reaction. The total protein concentration was determined using the Bradford method.

4.10. Evaluation of accumulation to tumor

PEG-uPA-NR and PEG-uPAscr-NR were intravenously injected into tumor-bearing mice (2 mM as gold atoms in 5% glucose solution, 10 μL/g of mouse weight). The mice were sacrificed 72 h after injection and tumors were collected. Quantitative analysis of the gold was performed using ICP-MS.

Acknowledgments

This research was supported by a Grant-in-Aid of Scientific Research (B) (No. 19300172) from the Japan Society for the Promotion of Science (JSPS) and by a grant for Precursory Research for Embryonic Science and Technology (PRESTO) from the Japan Science and Technology Agency (JST).

References and notes

1. Gullotti, E.; Yeo, Y. *Mol. Pharm.* **2009**, *6*, 1041.
2. Matsumura, Y.; Maeda, H. *Cancer Res.* **1986**, *46*, 6387.
3. Maeda, H.; Wu, J.; Sawa, T.; Matsumura, Y.; Hori, K. *J. Controlled Release* **2000**, *65*, 271.
4. Hirsch, L. R.; Stafford, R. J.; Bankson, J. A.; Sershen, S. R.; Rivera, B.; Price, R. E.; Hazle, J. D.; Halas, N. J.; West, J. L. *Proc. Natl. Acad. Sci. U.S.A.* **2003**, *23*, 13549.
5. Kirpotin, D. B.; Drummond, D. C.; Shao, Y.; Shalaby, M. R.; Hong, K.; Nielsen, U. B.; Marks, J. D.; Benz, C. C.; Park, J. W. *Cancer Res.* **2006**, *66*, 6732.
6. Huang, X.; El-Sayed, I. H.; Qian, W.; El-Sayed, M. A. *J. Am. Chem. Soc.* **2006**, *128*, 2115.
7. Wang, C.; Chen, J.; Talavage, T.; Irudayaraj, J. *Angew. Chem., Int. Ed.* **2009**, *48*, 2759.
8. Gabizon, A.; Horowitz, A. T.; Goren, D.; Tzemach, D.; Shmeeda, H.; Zalipsky, S. *Clin. Cancer Res.* **2003**, *9*, 6551.
9. Bartlett, D. W.; Su, H.; Hildebrandt, I. J.; Weber, W. A.; Davis, M. E. *Proc. Natl. Acad. Sci.* **2007**, *104*, 15549.
10. Xiong, X. B.; Huang, Y.; Lu, W. L.; Zhang, H.; Zhang, X.; Zhang, Q. *Pharm. Res.* **2005**, *22*, 933.
11. Li, Z.; Huang, P.; Zhang, X.; Lin, J.; Yang, S.; Liu, B.; Gao, F.; Xi, P.; Ren, Q.; Cui, D. *Mol. Pharm.* **2010**, *7*, 94.
12. Farokhzad, O. C.; Jon, S.; Khademhosseini, A.; Tran, T. N.; Lavan, D. A.; Langer, R. *Cancer Res.* **2004**, *64*, 7668.
13. Gerweck, L. E.; Seetharaman, K. *Cancer Res.* **1996**, *56*, 1194.
14. Lee, E. S.; Oh, K. T.; Kim, D.; Youn, Y. S.; Bae, Y. H. *J. Controlled Release* **2007**, *123*, 19.
15. Ko, J.; Park, K.; Kim, Y. S.; Kim, M. S.; Han, J. K.; Kim, K.; Park, R. W.; Kim, I. S.; Song, H. K.; Lee, D. S.; Kwon, I. C. *J. Controlled Release* **2007**, *123*, 109.
16. Min, K. H.; Park, K.; Kim, Y. S.; Bae, S. M.; Lee, S.; Jo, H. G.; Park, R. W.; Kim, I. S.; Jeong, S. Y.; Kim, K.; Kwon, I. C. *J. Controlled Release* **2008**, *127*, 208.
17. Chau, Y.; Tan, F. E.; Langer, R. *Bioconjugate Chem.* **2004**, *15*, 931.
18. Chau, Y.; Padera, R. F.; Dang, N. M.; Langer, R. *Int. J. Cancer* **2006**, *118*, 1519.
19. Chau, Y.; Dang, N. M.; Tan, F. E.; Langer, R. *J. Pharm. Sci.* **2006**, *95*, 542.
20. Hatakeyama, H.; Akita, H.; Kogure, K.; Oishi, M.; Nagasaki, Y.; Kihira, Y.; Ueno, M.; Kobayashi, H.; Kikuchi, H.; Harashima, H. *Gene Ther.* **2007**, *14*, 68.
21. Harris, T. J.; von Maltzahn, G.; Lord, M. E.; Park, J. H.; Agrawal, A.; Min, D. H.; Sailor, M. J.; Bhatia, S. N. *Small* **2008**, *4*, 1307.
22. Lee, S.; Cha, E. J.; Park, K.; Lee, S. Y.; Hong, J. K.; Sun, I. C.; Kim, S. Y.; Choi, K.; Kwon, I. C.; Kim, K.; Ahn, C. H. *Angew. Chem., Int. Ed.* **2008**, *47*, 2804.
23. Mok, H.; Bae, K. H.; Ahn, C. H.; Park, T. G. *Langmuir* **2009**, *25*, 1645.
24. Andreasen, P. A.; Egelund, R.; Petersen, H. H. *Cell. Mol. Life Sci.* **2000**, *57*, 25.
25. Kinoh, H.; Inoue, M. *Front. Biosci.* **2008**, *1*, 2327.
26. Kinoh, H.; Inoue, M.; Komaru, A.; Ueda, Y.; Hasegawa, M.; Yonemitsu, Y. *Gene Ther.* **2009**, *16*, 392.
27. Yu, Y. Y.; Chang, S. S.; Lee, C. L.; Wang, C. R. C. *J. Phys. Chem. B* **1997**, *101*, 6661.
28. Link, S.; Mohamed, M. B.; El-Sayed, M. A. *J. Phys. Chem. B* **1999**, *103*, 3073.
29. Weissleder, R. *Nat. Biotechnol.* **2001**, *19*, 316.
30. Chou, C. H.; Chen, C. D.; Wang, C. R. C. *J. Phys. Chem. B* **2005**, *109*, 11135.
31. Liao, L.; Hafner, J. H. *Chem. Mater.* **2005**, *17*, 4636.
32. Niidome, T.; Yamagata, M.; Okamoto, Y.; Akiyama, Y.; Takahashi, H.; Kawano, T.; Katayama, Y.; Niidome, Y. *J. Controlled Release* **2006**, *114*, 343.
33. Akiyama, Y.; Mori, T.; Katayama, Y.; Niidome, T. *J. Controlled Release* **2009**, *139*, 81.
34. Niidome, T.; Akiyama, Y.; Shimoda, K.; Kawano, T.; Mori, T.; Katayama, Y.; Niidome, Y. *Small* **2008**, *4*, 1001.
35. Eghtedari, M.; Oraevsky, A.; Copland, J. A.; Kotov, N. A.; Conjusteau, A.; Motamedi, M. *Nano Lett.* **2007**, *7*, 1914.
36. Dickerson, E. B.; Dreaden, E. C.; Huang, X.; El-Sayed, I. H.; Chu, H.; Pushpanketh, S.; McDonald, J. F.; El-Sayed, M. A. *Cancer Lett.* **2008**, *269*, 57.
37. Niidome, T.; Akiyama, Y.; Yamagata, M.; Kawano, T.; Mori, T.; Niidome, Y.; Katayama, Y. *J. Biomater. Sci., Polym. Ed.* **2009**, *20*, 1203.
38. Niidome, Y.; Nishioka, K.; Kawasaki, H.; Yamada, S. *Chem. Commun.* **2003**, *18*, 2376.